Measurements of the Composition and Molecular Weight Dependence of the Flory−Huggins Interaction Parameter

Alisyn J. Nedoma,[†] Megan L. Robertson,[†] Nisita S. Wanakule,[†] and Nitash P. Balsara*[,†,‡,§]

Department of Chemical Engineering, University of California, Berkeley, California 94720; Materials Sciences Division, Lawrence Berkeley National Laboratory, Berkeley, California 94720; and Environmental Energy Technologies Division, Lawrence Berkeley National Laboratory, Berkeley, California 94720

Received March 28, 2008; Revised Manuscript Received May 7, 2008

ABSTRACT: The phase behavior of binary blends of polyolefins is studied using small-angle neutron scattering. Component 1 is polyisobutylene (PIB), and component 2 is deuterated polybutadiene (dPB). Blends of these polymers are known to exhibit lower critical solution temperatures. The scattering intensity profiles from homogeneous PIB/dPB blends are fit to the random phase approximation to determine χ, the Flory−Huggins interaction parameter. We demonstrate that χ depends on temperature, blend composition, and component molecular weights.

Introduction

The Flory−Huggins theory continues to be the starting point for quantifying the interactions between chemically dissimilar polymer chains.[1,2] The attractive feature of this theory is that knowledge of a single parameter, χ, enables the determination of the thermodynamic properties of any binary polymer blend, regardless of the molecular weights of the components or the blend composition. In theory, χ is related to the local energetic interactions between monomers in the system. In practice, χ is an experimentally determined quantity. A large majority of the more recent determinations of χ are based on small-angle neutron scattering (SANS).[3–9] In these experiments, the measured scattering profiles of single phase polymer blends, which reflect the magnitude of concentration fluctuations, are fit to theoretical predictions based on the random phase approximation (RPA), originally derived by de Gennes.[10]

The Flory−Huggins theory prediction of the free energy per unit volume for mixing two polymers labeled 1 and 2, ΔG_m, is

$$\frac{\Delta G_m v}{kT} = \frac{\phi_1 \ln \phi_1}{N_1} + \frac{(1-\phi_1)\ln(1-\phi_1)}{N_2} + \chi\phi_1(1-\phi_1) \quad (1)$$

where ϕ_1 is the volume fraction of component 1 in the mixture, v is a reference volume which we set equal to 0.1 nm^3, k is the Boltzmann constant, T is the absolute temperature, and N_i is the number of repeat units per chain of type i ($i = 1, 2$), where each repeat unit is assumed to have a volume equal to v. We compute N_i using

$$N_i = \frac{\hat{N}_i v_i}{v} \quad (2)$$

where $\hat{N}_i$ is the number of chemical repeat units in chain i and v_i is the volume of each chemical repeat unit. Classical thermodynamics can be used to predict phase diagrams in polymer blends on the basis of eq 1 if we assume that χ is only a function of T (we limit this paper to a discussion of thermodynamics at atmospheric pressure) and is independent of either blend composition or molecular weight. For a blend obeying Flory−Huggins theory, the volume fraction of component 1 at the critical point is given by

$$\phi_{1c} = \frac{1}{1 + (N_1/N_2)^{1/2}} \quad (3)$$

and the value of χ at the critical point is given by

$$\chi_c = \frac{2}{N_{AVE}} \quad (4)$$

where N_{AVE} is defined as

$$N_{AVE} = 4\left[\frac{1}{N_1^{1/2}} + \frac{1}{N_2^{1/2}}\right]^{-2} \quad (5)$$

Limitations of the Flory−Huggins theory have been noted by theoreticians and experimentalists alike.[11–15] The fact that two parameter models are needed to describe the thermodynamics of small molecule mixtures is well-established.[16] It is thus clear that a quantitative understanding of polymer blend thermodynamics will require more sophisticated theories that go beyond the one parameter Flory−Huggins theory. There is, however, no consensus on how to improve upon the Flory−Huggins theory.

It is our view that our limited understanding of the thermodynamics of polymer blends is due to experimental as well as theoretical limitations. Miscibility in polymer systems is limited to the regime where $\chi < 2/N_{AVE}$, and thus when N_{AVE} is large, χ is small in the miscible region. If χ decreases with increasing temperature, which is the case for most polymer pairs, then the blend exhibits upper critical solution temperature (UCST) behavior. In such cases the range of N_{AVE} values over which χ can be measured is extremely limited. Single-phase blends at the critical composition are best suited for measuring χ because of the presence of large concentration fluctuations, which, in turn, give rise to large SANS signals. In this regime, small changes in χ lead to large changes in predicted scattering [RPA], and thus scattering measurements can lead to extremely accurate estimates of χ. It is thus not surprising that a large majority of the values of χ in the literature are based on measurements obtained from a single polymer blend with a carefully chosen value of N_{AVE} in the vicinity of the critical point.[12,14,15,17] The SANS profiles obtained from single-phase blends well-removed

* To whom correspondence should be addressed: e-mail nbalsara@berkeley.edu, Ph 510.642.8937, Fax 510 0.642.4778.
† University of California, Berkeley.
‡ Materials Sciences Division, Lawrence Berkeley National Laboratory.
§ Environmental Energy Technologies Division, Lawrence Berkeley National Laboratory.

10.1021/ma800698r CCC: $40.75
Published on Web 07/02/2008

from the critical point are difficult to analyze because the signal in these systems is dominated by scattering from individual chains and is thus not sensitive to changes in χ. Small errors in determination of factors such as chain length, chain polydispersity, and labeling heterogeneity[17] can lead to large errors in the experimentally determined χ. Thus, values of χ determined from off-critical polymer blends are usually accompanied by large error bars.[4,14,18,19] On the theoretical side, it is challenging to model systems wherein the differences between the energies of monomer−monomer interactions are of order kT/N_{AVE}, especially when N_{AVE} is large, and the interactions of interest are orders of magnitude smaller than kT. It is obvious that reliable measurements of χ over a wide range of ϕ_1, N_1, and N_2 values are needed at this juncture.

The purpose of this paper is to describe results obtained from experiments conducted to address this need. When χ is less than zero, single phase systems are obtained regardless of ϕ_1, N_1, and N_2. If the blend exhibits lower critical solution temperature (LCST) behavior, χ increases with temperature, and if χ exceeds $2/N_{AVE}$ at an accessible temperature, then the region of critical fluctuations can be accessed, and SANS can be used to measure χ over a wide range of ϕ_1, N_1, and N_2. The system chosen for our study was thus polyisobutylene (component 1) and saturated polybutadiene with 63% 1,2-addition (component 2), which exhibits LCST behavior. Nine blends were prepared at the Flory−Huggins critical composition, ϕ_{1c}, as predicted by eq 3, with N_{AVE} values ranging from 208 to 1750. This enables determination of the composition (ϕ_1) dependence of χ using data obtained from critical blends only. The results of experiments on these blends indicated that the measured χ parameter depends on ϕ_1. This is not surprising because many (if not all) previous studies on LCST blends have shown that the χ parameter depends on composition in these systems.[20–22] However, the critical composition, ϕ_{1c}, of the blends that we studied was calculated assuming that χ is independent of composition. There are no simple formulas for computing the critical composition of blends where χ depends on composition. In fact, we show that the critical composition can only be readily calculated for blends that have accessible critical points. This is due to our inability to extrapolate χ to temperatures outside the range of our measurements. The phase separation temperature was accessible in only four out of the nine blends studied. For each of these four systems, we prepared two additional blends: one with a composition $\phi_1 = \phi_{1cc}$, where ϕ_{1cc} is the calculated critical composition based on an educated guess[23] for the composition dependence of χ, and another with composition $\phi_1 = 1 - \phi_{1cc}$, which we expect to be well-removed from the critical point. We conclude this paper by reporting an expression for χ that is consistent with all of the measurements. To our knowledge, this study represents the most comprehensive measurement of χ in any polymer blend system. We make no attempt to provide a molecular interpretation for the measured dependence of χ on ϕ_1, N_1, and N_2.

Experimental Section

Butadiene was polymerized anionically using techniques described in ref 24 to yield polybutadiene with 63% 1,2-addition. The C=C double bonds of the resulting polybutadiene were saturated under high pressure using deuterium gas to yield partially deuterated polybutadiene. Polyisobutylene was synthesized via cationic polymerization, also described in ref 24. The characteristics of the homopolymers used in this study are listed in Table 1. The level of deuteration of the dPB samples varies by about 20%. On the basis of previous studies of the effect of deuteration on thermodynamics,[25–28] we do not expect the differences in deuteration level to affect blend thermodynamics.

Binary blends were prepared according to the methods described in ref 24. Component 1 is PIB, and component 2 is dPB. Samples were pressed into a 1 mm thick aluminum spacer with inner diameter 14 mm and annealed under vacuum atop a 1 mm thick quartz disk for 48 h at 90 °C. A second quartz disk was then placed on top of the spacer, and the edges were sealed with epoxy, leaving a small gap for the excess polymer (due to thermal expansion) to leak out of the sample cell at elevated temperatures. The sample was annealed for an additional 10 min at 90 °C. Table 2 lists components, N_{AVE}, and ϕ_1 of the blends prepared. The letter in the name of each blend indicates the composition of the blend (the code will de described shortly) while the number in the name gives N_{AVE}.

Table 1. Characterization of Homopolymers[a]

name	M_w (kg/mol)	PDI	ρ (g/mL)	N	n_D
PIB(13)	12.5	1.04	0.9134	227	NA
PIB(45)	44.6	1.04	0.9140	810	NA
PIB(57)	56.8	1.02	0.9144	1031	NA
dPB63(10)	10.5	1.02	0.9125	191	3.44
dPB63(58)	62	1.01	0.9187	1120	3.65
dPB63(187)	197.2	1.02	0.9123	3589	3.04

[a] M_w is the weight-averaged molecular weight (for deuterated species the weight in parentheses is that of the hydrogenated analogue); PDI is the polydispersity index M_w/M_n, where M_n is the number-averaged molecular weight; ρ is the average density measured using a density gradient column; N is the number of reference volumes comprising a single chain; and n_D is the average number of deuterium atoms per C_4 repeat unit.

Table 2. Composition of Binary Blends Used To Measure χ_{sc}[a]

blend	component 1	component 2	N_{AVE}	ϕ_1
F(373)	PIB(57)	dPB63(10)	373	0.301
F(346)	PIB(45)	dPB63(10)	346	0.327
F(208)	PIB(13)	dPB63(10)	208	0.478
F(1075)	PIB(57)	dPBD(58)	1075	0.510
F(947)	PIB(45)	dPBD(58)	947	0.540
F(1750)	PIB(57)	dPBD(187)	1750	0.651
F(1489)	PIB(45)	dPBD(187)	1489	0.678
F(432)	PIB(13)	dPB63(58)	432	0.690
F(580)	PIB(13)	dPB63(187)	580	0.799
C(1075)	PIB(57)	dPBD(58)	1075	0.233
C(1750)	PIB(57)	dPBD(187)	1750	0.238
C(947)	PIB(45)	dPBD(58)	947	0.267
C(1489)	PIB(45)	dPBD(187)	1489	0.272
A(1489)	PIB(45)	dPBD(187)	1489	0.728
A(947)	PIB(45)	dPBD(58)	947	0.733
A(1750)	PIB(57)	dPBD(187)	1750	0.762
A(1075)	PIB(57)	dPBD(58)	1075	0.767

[a] Blends are denoted by a letter corresponding to the blend series (F, C, or A) followed by the average molecular weight, N_{AVE}, in parentheses.

Small-angle neutron scattering (SANS) measurements were made on beamlines NG3 and NG7 at the National Institute of Standards and Technology in Gaithersburg, MD. The raw data were corrected for detector sensitivity, background, empty cell scattering, incoherent scattering, and contributions due to nonuniform deuteration using standard methods[29] and integrated azimuthally to determine absolute coherent scattering intensity, I, vs magnitude of the scattering vector, q ($q = 4\pi \sin(\theta/2)/\lambda$, where θ is the scattering angle and λ is the wavelength of the incident beam).

Experimental Discussion

The random-phase approximation (RPA) gives the following expression for the coherent SANS profile, $I(q)$:[10]

$$I(q) = \left(\frac{b_1}{v_1} - \frac{b_2}{v_2}\right)^2 \frac{1}{v}\left[\frac{1}{N_1\phi_1 P_1(q)} + \frac{1}{N_2\phi_2 P_2(q)} - 2\chi_{sc}\right]^{-1} \quad (6)$$

We use the symbol χ_{sc} to represent χ determined from SANS, b_i is the neutron scattering length of monomer i, v_i is the volume of the monomer used to determine b_i, and $P_i(q)$ is the single chain form factor for species i, given by the Debye function

$$P_i(q) = \frac{2}{\left(q^2 R_{g,i}^2\right)^2}\{\exp[-(qR_{q,i})^2] + (qR_{q,i})^2 - 1\} \quad (7)$$

where $R_{g,i}$ is the radius of gyration of a chain of species i and

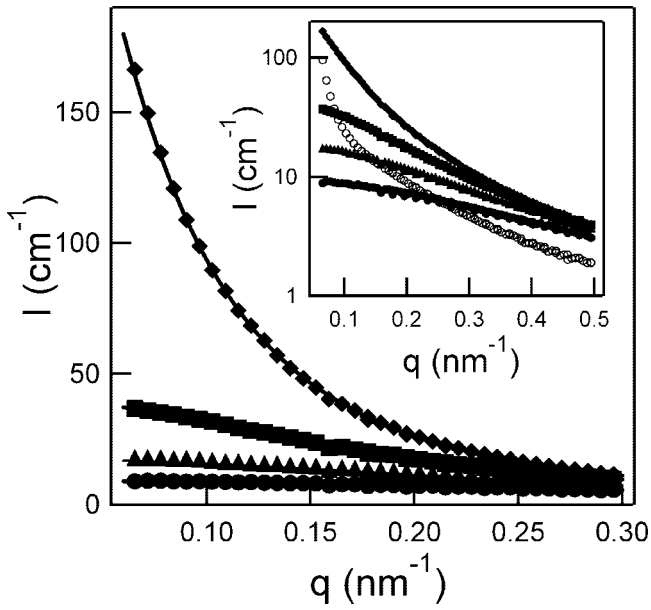

Figure 1. SANS intensity, I, vs magnitude of the scattering vector, q, for blend F(947) at the following temperatures: 303 (●), 343 (▲), 383 (solid triangle pointing right), and 423 K (♦). The solid curves are RPA fits to the scattering profiles. The inset shows the same scattering profiles on a logarithmic scale as well as the profile at 463 K (○) when the blend is phase separated.

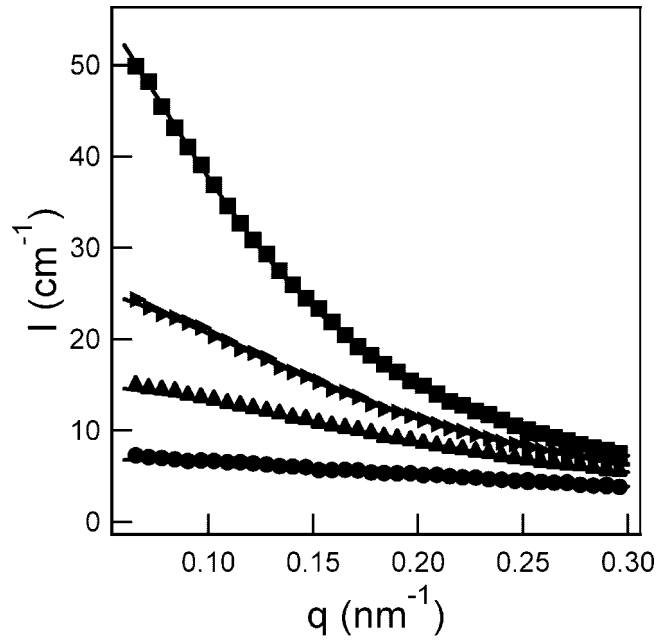

Figure 2. SANS profiles I vs q at selected temperatures within the single phase window for blend F(1750) with composition $\phi_{1c} = 0.651$. The temperatures shown are 303 K (●), 343 K (▲), 363 K (solid triangle pointing right), and 383 K (■). The solid curves are RPA fits to the data.

is related to the statistical segment length of a chain of type i, l_i, by $R_{g,i}^2 = N_i l_i^2/6$. N_i and χ are based on a 0.1 nm^3 reference volume. Following previously established procedures,[23,24,30] the measured $I(q)$ is fit to eq with two fitting parameters: χ and α, where $\alpha = l_1(T)/l_{1,std} = l_2(T)/l_{2,std}$, where $l_{i,std}$ are the nominal values for the statistical segment lengths established in the literature; $l_{1,std}$ and $l_{2,std}$ are 0.58 and 0.75 nm, respectively.[24] Error in the measurement of χ derives from error in the measured intensity (1%), error in the incoherent signal subtraction (1−6%), and errors in the measurement of homopolymer molecular weight (5−10%). The resultant error in χ is expected to be less than 15%.

We first begin by discussing results obtained from the F-series of blends (Table 2). The composition of the F-series blends was calculated using eq 3, i.e., the critical composition based on Flory−Huggins theory with a composition-independent χ parameter. A subset of these data were reported previously in ref 23. In Figure 1 we show typical RPA fits through the SANS data obtained from blend F(947) at selected temperatures between 303 and 423 K. This is a symmetric blend with $N_1 \approx N_2$ and $\phi_1 = 0.540$. The RPA fits enable determination of the temperature dependence of χ_{sc}. The inset of Figure 1 compares SANS profiles obtained in the 303−423 K range with that obtained at 463 K. The qualitative differences between the 463 K data and the lower temperature data at both low and high q is due to macroscopic phase separation, as established in previous studies.[22,31] The RPA can only be applied to homogeneous blends, so our measurements of χ_{sc} are limited to the 303−423 K range for blend F(947). In the discussions that follow, we limit our attention to blends that are homogeneous. It is important to note that $I(q)$ of F(947) is a sensitive function of temperature, especially as the phase separation temperature is approached. This is the scattering signature of a single phase blend approaching a critical point. In Figure 2 we show the SANS scattering profiles for blend F(1750) at selected temperatures. As was the case with F(947) data, $I(q)$ in this case is also a sensitive function of temperature, especially as the phase separation temperature (397 K) is approached. It is evident that this asymmetric blend with $N_1 = 1031$, $N_2 = 3589$, and $\phi_1 = \phi_{1c} = 0.651$ also exhibits the scattering signature of a single phase blend approaching a critical point. Figure 3 shows the scattering profiles for blend F(432). This is an asymmetric blend with $N_1 = 227$, $N_2 = 1120$, and $\phi_1 = \phi_{1c} = 0.690$. Unlike F(1750), the phase separation temperature of blend F(432) is above the upper limit of our temperature window. Thus, SANS data from this blend can be used to obtain χ_{sc} over the entire accessible temperature window from 303 to 474 K. The solid curves in Figures 2 and 3 are RPA fits through the data. It is clear from Figures 1–3 that the two parameter RPA fits are consistent with all of the features seen in the data.

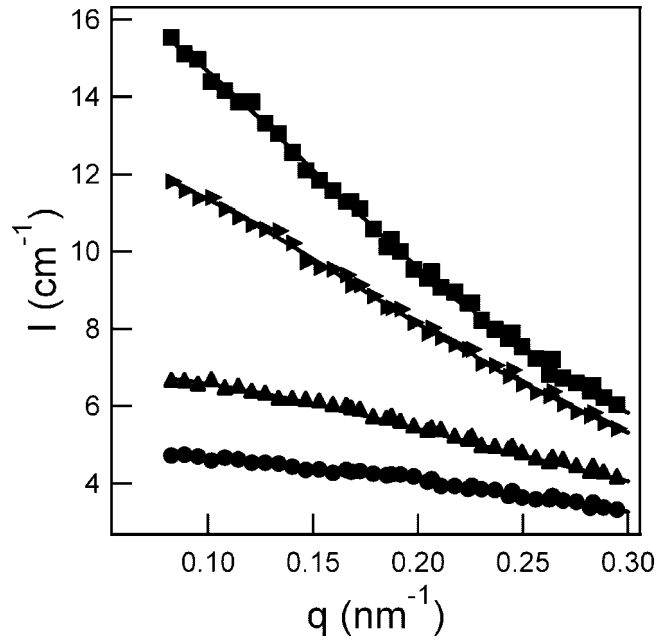

Figure 3. SANS profiles I vs q at selected temperatures for single phase blend F(432), an asymmetric blend with $\phi_{1c} = 0.690$. The temperatures shown are 302 K (●), 342 K (▲), 423 K (solid triangle pointing right), and 474 K (■). The solid lines are RPA fits to the data.

The general observations reported in Figures 1–3 hold for all of the F-series blends. For F(947), F(1075), F(1489) and F(1750), the phase separation temperatures were below the upper limit of the SANS sample holder. For F(208), F(346), F(373), F(432), and F(580) the phase separation temperatures were above the upper limit of the SANS sample holder.

Not unexpectedly, we find that the χ parameters obtained from the F-series blends at a given temperature differ substantially from one another. For example, at 303 K, χ_{sc} of F(580) is $-0.005\,45$ while that of F(373) is $-0.003\,12$. It is not clear whether the difference between the χ_{sc} parameters obtained from F(580) and F(373) is due to differences in ϕ_1 or N_{AVE}. We made an educated guess that χ_{sc} for our system was independent of N_{AVE} and depended only on ϕ_1. By fitting the measured χ_{sc} values from the F-series, we obtained the composition dependence of χ, and using standard thermodynamic equations,[32] we obtained new estimates of the critical composition of blends PIB(57)/PB(187), PIB(45)/PB(187), PIB(57)/PB(58), and PIB(45)/PB(58). We refer to this composition as ϕ_{1cc}. For these blends with accessible phase separation temperatures, we prepared two additional series of blends: the C-series with $\phi_1 = \phi_{1cc}$ and the A-series with $\phi_1 = 1 - \phi_{1cc}$. The compositions of the C- and A-series blends are given in Table 2.

In Figure 4a,b, we show the SANS profiles obtained from A(947) and C(947) at selected temperatures with the corresponding RPA fits. As was the case with the F-series, the RPA fits capture all aspects of the SANS profiles. This was true for all the C- and A-series blends.

In Figure 5 we show RPA fit values of α at 303 and 383 K for all of the blends studied as a function of $(2\phi_1 - 1)$. $(2\phi_1 - 1)$ is a convenient measure of blend composition as it is zero for symmetric blends with $\phi_1 = 0.5$, and most measurements of χ_{sc} in the literature are made using symmetric blends. The values of α range between 1.0 and 0.7. There is not a systematic dependence of α either on temperature or ϕ_1. The values of α are reported here mainly for completeness, and we do not discuss them further.

In Figure 6 the solid markers show the RPA values of χ_{sc} at 303, 343, and 383 K as a function of blend composition. Errors in the measured values of χ are expected to be within 4−15%.[22] It is clear that χ_{sc} increases with increasing temperature and decreases with increasing $2\phi_1 - 1$. However, it is also clear that any simple function of temperature and composition is incapable of capturing all of the features of the χ measurements seen in Figure 6. For example, blends A(947) and A(1489) have a similar composition with $(2\phi_1 - 1) = 0.466$ and 0.456, respectively. However, χ_{sc} values for these blends, $-0.003\,90$ for A(947) and $-0.004\,87$ for A(1489), differ substantially from each other. We were thus forced to examine expressions for χ_{sc} that depend on temperature, composition, and molecular weight. We examined several expressions and settled on the following expression for χ_{sc}.

$$\chi_{sc} = A_{sc}(T) + B_{sc}(T)\frac{2\phi_1 - 1}{N_{AVE}} \tag{8}$$

with A_{sc} and B_{sc} as fitting parameters. Of all of the empirical equations that we tried, eq 8 provided the lowest average standard deviation between the proposed equation and experimental data. It also had the simplest functional form. The open markers in Figure 6 show the fit values of χ_{sc} for all blends at selected temperatures. It is clear from Figure 6 that much of the complexity seen in the measurements of χ_{sc} is consistent with eq 8. The temperature dependence of A_{sc} and B_{sc} parameters that minimize the standard deviation between the measurements and eq 8 is shown in parts a and b of Figure 7, respectively.

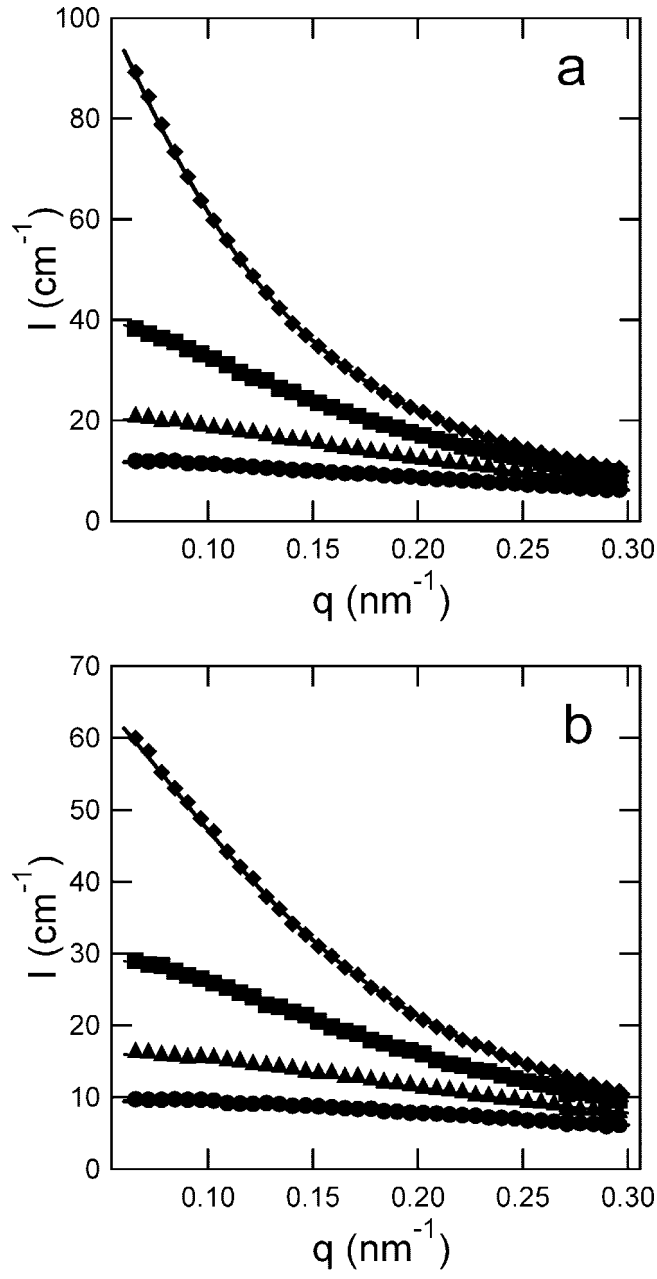

Figure 4. SANS intensity, I, vs magnitude of the scattering vector, q, at the following temperatures: 303 (●), 343 (▲), 383 (■), and 423 K (♦) for (a) blend C(947) and (b) blend A(947). The solid curves are RPA fits to the scattering profile.

Both $A_{sc}(T)$ and $B_{sc}(T)$ were assumed to be quadratic functions of $1/T$, and the resulting least-squares fits are the curves in Figure 7. The final expression for χ_{sc} is

$$\chi_{sc} = -0.00622 + \frac{10.6}{T} - \frac{3040}{T^2} + \left[-2.17 + \frac{1910}{T} - \frac{687100}{T^2}\right]\left[\frac{2\phi_1 - 1}{N_{AVE}}\right] \tag{9}$$

Figure 8a−c compares the predicted χ_{sc} with the measured χ_{sc} as a function of temperature for three blend compositions all with the same N_{AVE}: C(947), F(947), and A(947) with $\phi_1 = 0.267$, 0.540, and 0.733, respectively. While deviations between eq 9 and the data are evident, the important features of the experimental data are captured by the proposed equation.

The inclusion of N_{AVE} in our expression for χ_{sc} (eq 8) is essential for fitting the data. Figure 9 shows a plot of χ_{sc} vs $(2\phi$

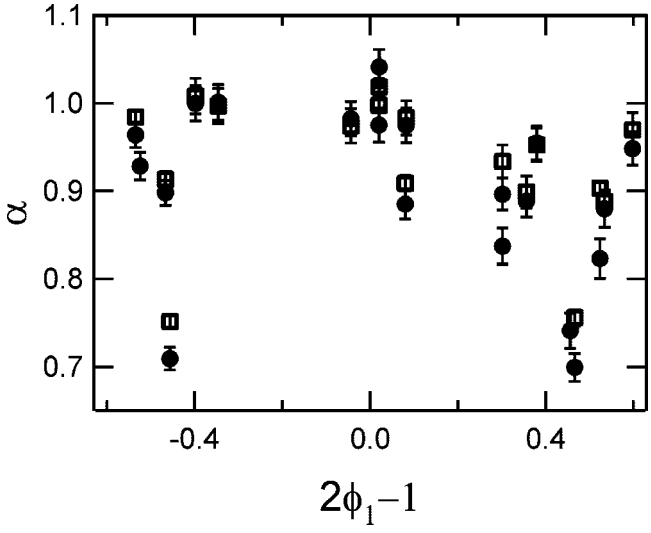

Figure 5. Composition dependence of the RPA fit parameter α for all blends at 303 (●) and 383 K (■).

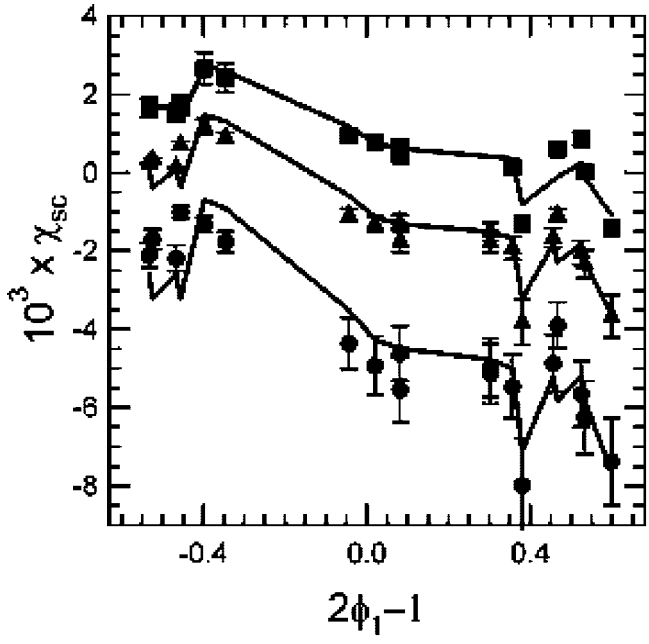

Figure 6. SANS measured values for χ_{sc} at selected temperatures: 303 (●), 343 (▲), and 383 K (■). The solid lines are the calculated values, using eq 9. The composition of each blend is unique. Thus, Table 2 can be used identify the homopolymer components in a particular blend.

$- 1)/N_{AVE}$. The data when plotted in this manner are approximately linear as expected. The least-squares linear fits through the data in Figure 9 give additional estimates of A_{sc} and B_{sc}. In Table 3 the values of A_{sc} and B_{sc} from Figure 9 are compared to those calculated from eq 9. We see excellent agreement between the two methods for estimating A_{sc} and B_{sc}.

When χ_{sc} is dependent on composition, we must differentiate the value measured with SANS from the parameter used in the Flory−Huggins equation to predict phase behavior, χ. The two parameters are interrelated by the derivatives of free energy as shown by Sanchez.[32]

$$\chi = \phi_2\chi_{\mu 1} + \phi_1\chi_{\mu 2} \tag{10}$$

where $\chi_{\mu 1}$ and $\chi_{\mu 2}$ are given by

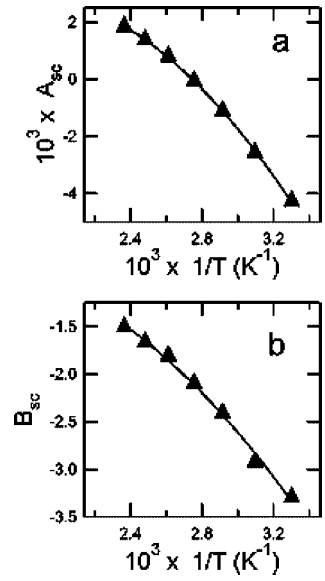

Figure 7. Temperature dependence of the fitting parameters for $\chi_{sc} = A_{sc}(T) + B_{sc}(T)[(2\phi_1 - 1)/N_{AVE}]$ with (a) A_{sc}; the solid curve fit is given by $A_{sc}(T) = -0.00622 + 10.6/T - 3040/T^2$ and (b) B_{sc}; the solid curve fit is given by $B_{sc}(T) = -2.17 + 1910/T - 687000/T^2$.

$$\chi_{\mu 1} = \frac{2}{(1-\phi_1)^2}\int_0^{\phi_2}(1-\phi'_1)\chi_{sc}\,d(1-\phi'_1)$$

$$\chi_{\mu 2} = \frac{2}{\phi_1^2}\int_0^{\phi_1}\phi'_1\chi_{sc}\,d\phi'_1 \tag{11}$$

It is straightforward to show that if χ_{sc} is a linear function of $(2\phi_1 - 1)$, then χ is also a linear function of $(2\phi_1 - 1)$. Employing eqs 8, 10, and 11, we obtain

$$\chi = A(T) + B(T)\frac{2\phi_1 - 1}{N_{AVE}} \tag{12}$$

where

$$A = A_{sc} = -0.00622 + \frac{10.6}{T} - \frac{3040}{T^2} \tag{13}$$

and

$$B = \frac{B_{sc}}{3} = -0.722 + \frac{638}{T} - \frac{229000}{T^2} \tag{14}$$

The relationship between χ and χ_{sc} is depicted in Figure 10, where results obtained from all of the blends at 303 K are shown. The true χ parameters exhibit a weaker dependence on composition and molecular weight than χ_{sc}. It is important to note, however, that the modest dependence of χ on ϕ_i and N_{AVE} seen in Figure 10 has a profound effect on the phase behavior of PIB/dPB blends.

The composition dependence of χ exhibited by these blends requires recalculation of the critical composition. The second and third derivatives of the Flory−Huggins free energy are zero value at the critical point, yielding two equations that must be solved simultaneously for revised estimates of the two unknown values: the critical composition $\phi_{1c,rev}$ and the critical temperature, $T_{c,rev}$.

$$\frac{\partial^2 G}{\partial\phi_1^2} = \frac{1}{N_1\phi_1} + \frac{1}{N_2(1-\phi_1)} + \frac{6B(T)(1-2\phi_1)}{N_{AVE}} - 2A(T) = 0$$

$$\frac{\partial^3 G}{\partial\phi_1^3} = -\frac{1}{N_1\phi_1^2} + \frac{1}{N_2(1-\phi_1)^2} - \frac{12B(T)}{N_{AVE}} = 0 \tag{15}$$

The revised values for the critical composition and critical temperature, $\phi_{1c,rev}$ and $T_{c,rev}$, for the PIB/dPB blends thus

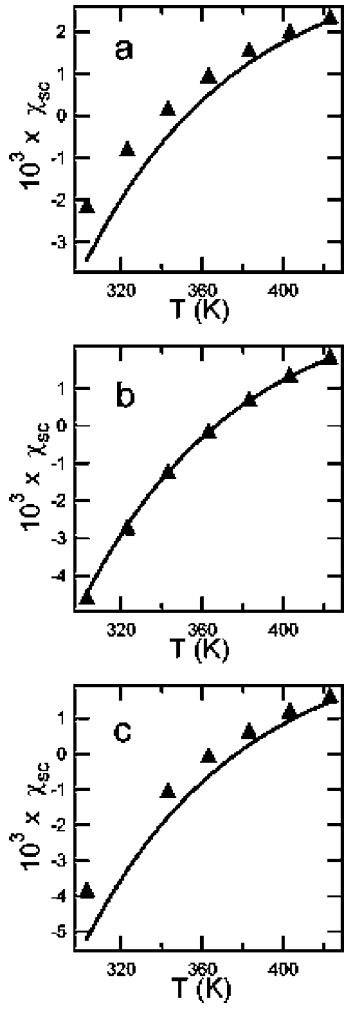

Figure 8. Predicted values of χ_{sc} according to eq 9 (solid curve) compared with measured values of χ_{sc} (▲) for blends (a) C(947), (b) F(947), and (c) A(947).

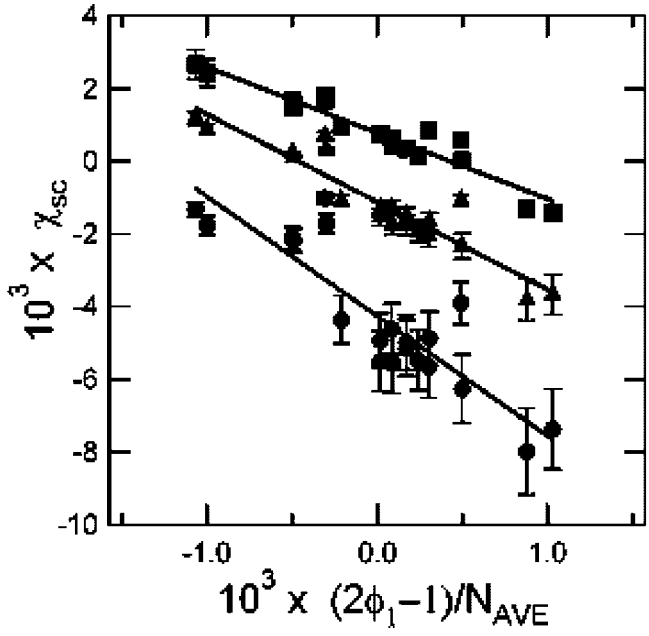

Figure 9. SANS measured values of χ_{sc} vs $(2\phi_1 - 1)/N_{AVE}$ at selected temperatures: 303 (●), 343 (▲), and 383 K (■). The solid lines are linear least-squares fits to the data with slopes and intercepts corresponding to B_{sc} and A_{sc}, respectively; values are reported in Table 3.

Table 3. A_{sc} and B_{sc} at Selected Temperatures[a]

	A_{sc}		B_{sc}	
T (K)	Figure 9	eq 9	Figure 9	eq 9
303	−0.004 27	−0.004 30	−3.29	−3.34
343	−0.001 12	−0.001 20	−2.41	−2.49
383	0.000 78	0.000 76	−1.81	−1.86

[a] A_{sc} and B_{sc} are determined in two different ways: (1) from Figure 9 A_{sc} is given by the intercept of the linear fit to χ_{sc} vs $(2\phi_1 - 1)/N_{AVE}$, and B_{sc} is given by the slope, and (2) by minimizing the standard deviation between eq 9 and experimental data.

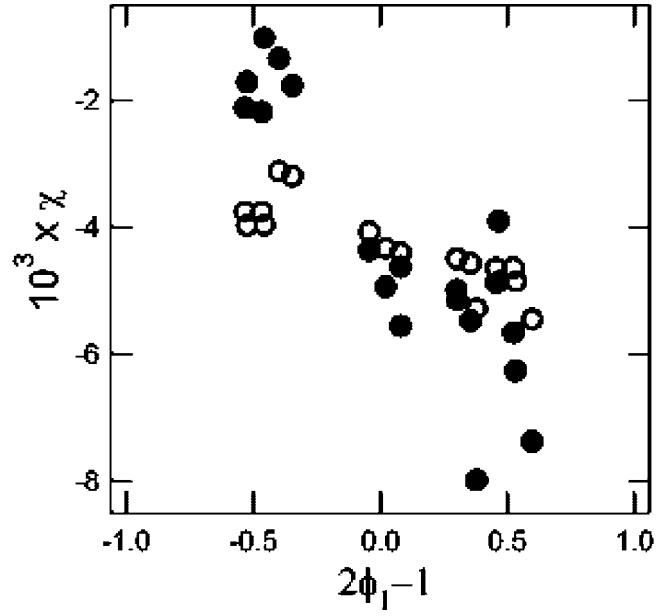

Figure 10. Flory−Huggins χ parameters calculated from eq 12 (○) compared with measured values of χ_{sc} from SANS experiments (●) at 303 K.

Table 4. Critical Points Predicted by Flory−Huggins Theory[a]

component 1	component 2	ϕ_{1c}	$\phi_{1c,rev}$	$T_{c,rev}$ (K)	N_{AVE}
PIB(13)	dPB63(10)	0.478			208
PIB(45)	dPB63(10)	0.327			346
PIB(57)	dPB63(10)	0.301			373
PIB(13)	dPB63(58)	0.690			432
PIB(13)	dPB63(187)	0.799			580
PIB(45)	dPB(58)	0.541	0.369	419	947
PIB(57)	dPB(58)	0.510	0.339	407	1075
PIB(45)	dPB(187)	0.678	0.467	404	1489
PIB(57)	dPB(187)	0.651	0.438	395	1750

[a] ϕ_{1c} is the critical point predicted from eq using the composition-independent χ given in ref 23, $\phi_{1c,rev}$ and $T_{c,rev}$ represent the critical point predicted from simultaneously solving eqs 15 where the composition and molecular weight dependence of χ is accounted for. A blank indicates eqs 15 do not lead to a convergent solution given the expression for χ (eq 9).

obtained are listed in Table 4 alongside the Flory−Huggins prediction for the critical composition, ϕ_{1c}. There is a significant difference between $\phi_{1c,rev}$ and ϕ_{1c}, indicating the importance of measuring χ as a function of both molecular weight and composition and differentiating between the measured interaction parameter, χ_{sc}, and the thermodynamic parameter χ. Experimentally, phase separation was not observed for five blends, as described earlier, because temperatures of phase separation exceeded the limit of the SANS holder. For these blends we tried to solve eqs 15 with the hope that the temperature dependences of the χ parameter given in eq 12 could be extrapolated to temperatures above those measured experimentally. However, none of these calculations converged, suggesting that the revised form of the proposed Flory−Huggins

free energy equation cannot be used at temperatures outside the temperature range of our experiments.

A final note concerns our determination of ϕ_{1cc}, the compositions used for the C-series blends. These compositions were obtained by solving eqs 15 with composition-dependent χ parameters obtained from the F-series blends only. The results of these experiments were reported in ref 23. It is evident that determining the true critical points of blends with χ parameters that depend on both composition and molecular weight is an iterative process. It is not clear, for example, if the equation that we have proposed for χ_{sc}, eq 8, will be consistent with future measurements of χ between PIB and dPB. Further work is need to determine whether $\phi_{1c,rev}$ and $T_{c,rev}$ represent the true critical points of the blends.

Conclusions

The temperature dependence of the χ parameter between saturated polybutadiene and polyisobutylene was measured over an unprecedented range of composition and component molecular weights. The most important conclusion of this study is that χ of this system depends on both ϕ_1 and N_{AVE}. A simple form for the dependence of χ on ϕ_1 and N_{AVE} is proposed and shown to be consistent with the measured data. In future work we will try to understand the reason for departures from the Flory−Huggins theory by comparing our data with theories that address a dependence of χ on N_{AVE}.[33–36] We will also attempt to clarify the location of the critical points in polyisobutylene/polybutadiene blends by conducting SANS and light scattering on blends with accessible phase separation temperatures over a wider range of compositions.

Acknowledgment. We acknowledge the support of the National Institute of Standards and Technology, U.S. Department of Commerce, in providing the neutron research facilities used in this work. This material is based on work supported by the National Science Foundation under Grants 0305711 and 0504122 and by NSF NIRT (No. EEC-034730). A.J.N. gratefully acknowledges the graduate researcher fellowship from Tyco Electronics.

References and Notes

(1) Flory, P. J. *Curr. Contents/Phys. Chem. Earth Sci.* **1985**, 18.
(2) Huggins, M. L. *Polym. J.* **1973**, *4*, 511–516.
(3) Kim, J. K.; Jang, J.; Lee, D. H.; Ryu, D. Y. *Macromolecules* **2004**, *37*, 8599–8605.
(4) Lee, J. H.; Balsara, N. P.; Chakraborty, A. K.; Krishnamoorti, R.; Hammouda, B. *Macromolecules* **2002**, *35*, 7748–7757.
(5) Lee, J. S.; Foster, M. D.; Wu, D. T. *Macromolecules* **2006**, *39*, 5113–5121.
(6) Lefebvre, A. A.; Balsara, N. P.; Lee, J. H.; Vaidyanathan, C. *Macromolecules* **2002**, *35*, 7758–7764.
(7) Tucker, R. T.; Han, C. C.; Dobrynin, A. V.; Weiss, R. A. *Macromolecules* **2003**, *36*, 4404–4410.
(8) Zirkel, A.; Gruner, S. M.; Urban, V.; Thiyagarajan, P. *Macromolecules* **2002**, *35*, 7375–7386.
(9) Ryu, D. Y.; Jeong, U.; Lee, D. H.; Kim, J.; Youn, H. S.; Kim, J. K. *Macromolecules* **2003**, *36*, 2894–2902.
(10) de Gennes, P. G. In *Scaling Concepts in Polymer Physics*; Cornell University Press: Ithaca, NY, 1979; p 109.
(11) Gujrati, P. D. *J. Chem. Phys.* **2000**, *112*, 4806–4821.
(12) Han, C. C.; Bauer, B. J.; Clark, J. C.; Muroga, Y.; Matsushita, Y.; Okada, M.; Qui, T. C.; Chang, T. H.; Sanchez, I. C. *Polymer* **1988**, *29*, 2002–2014.
(13) Wang, Z. G. *J. Chem. Phys.* **2002**, *117*, 481–500.
(14) Krishnamoorti, R.; Graessley, W. W.; Balsara, N. P.; Lohse, D. J. *J. Chem. Phys.* **1994**, *100*, 3894–3904.
(15) Bates, F. S.; Muthukumar, M.; Wignall, G. D.; Fetters, L. J. *J. Chem. Phys.* **1988**, *89*, 535–544.
(16) Prausnitz, J. M.; Lichtenthaler, R. N.; Asevedo, E. G. d. *Molecular Thermodynamics of Fluid-Phase Equilibria*, 2nd ed.; Prentice-Hall: Englewood Cliffs, NJ, 1989.
(17) Balsara, N. P.; Lohse, D. J.; Graessley, W. W.; Krishnamoorti, R. *J. Chem. Phys.* **1994**, *100*, 3905–3910.
(18) Lin, C. C.; Jonnalagadda, S. V.; Balsara, N. P.; Han, C. C.; Krishnamoorti, R. *Macromolecules* **1996**, *29*, 661–669.
(19) Krishnamoorti, R.; Graessley, W. W.; Dee, G. T.; Walsh, D. J.; Fetters, L. J.; Lohse, D. J. *Macromolecules* **1996**, *29*, 367–376.
(20) Reichart, G. C.; Graessley, W. W.; Register, R. A.; Krishnamoorti, R.; Lohse, D. J. *Macromolecules* **1997**, *30*, 3036–3041.
(21) Krishnamoorti, R. *Rubber Chem. Technol.* **1999**, *72*, 580–586.
(22) Balsara, N. P.; Fetters, L. J.; Hadjichristidis, N.; Lohse, D. J.; Han, C. C.; Graessley, W. W.; Krishnamoorti, R. *Macromolecules* **1992**, *25*, 6137–6147.
(23) Nedoma, A. J.; Robertson, M. L.; Wanakule, N. S.; Balsara, N. P. *Ind. Eng. Chem. Res.* **2008**, in press.
(24) Reynolds, B. J.; Ruegg, M. L.; Balsara, N. P.; Radke, C. J.; Shaffer, T. D.; Lin, M. Y.; Shull, K. R.; Lohse, D. J. *Macromolecules* **2004**, *37*, 7401–7417.
(25) Londono, J. D.; Narten, A. H.; Wignall, G. D.; Honnell, K. G.; Hsieh, E. T.; Johnson, T. W.; Bates, F. S. *Macromolecules* **1994**, *27*, 2864–2871.
(26) Crist, B. *Macromolecules* **1998**, *31*, 5853–5860.
(27) Graessley, W. W.; Krishnamoorti, R.; Balsara, N. P.; Fetters, L. J.; Lohse, D. J.; Schulz, D. N.; Sissano, J. A. *Macromolecules* **1993**, *26*, 1137–1143.
(28) Wignall, G. D.; Bates, F. S. *Makromol. Chem., Macromol. Symp.* **1988**, *15*, 105–122.
(29) Kline, S. *SANS data reduction and analysis, version 4.2*; National Institute of Standards and Technology: Gaithersburg, MD, 2003.
(30) Ruegg, M. L.; Reynolds, B. J.; Lin, M. Y.; Lohse, D. J.; Balsara, N. P. *Macromolecules* **2006**, *39*, 1125–1134.
(31) Sakurai, S.; Jinnai, H.; Hasegawa, H.; Hashimoto, T.; Han, C. C. *Macromolecules* **1991**, *24*, 4839–4843.
(32) Sanchez, I. C. *Polymer* **1989**, *30*, 471–475.
(33) Taylor, J. K.; Debenedetti, P. G.; Graessley, W. W.; Kumar, S. K. *Macromolecules* **1996**, *29*, 764–773.
(34) TaylorMaranas, J. K.; Debenedetti, P. G.; Graessley, W. W.; Kumar, S. K. *Macromolecules* **1997**, *30*, 6943–6946.
(35) Hooper, J. B.; Schweizer, K. S. *Macromolecules* **2006**, *39*, 5133–5142.
(36) Cho, J. H. *Macromolecules* **2000**, *33*, 2228–2241.

MA800698R